Canadian Mineralogist
Vol. 29, pp. 943-963 (1991)

THE ROLE OF BIOTITE AS A CATALYST IN REACTION MECHANISMS THAT FORM SILLIMANITE

CHARLES T. FOSTER, JR.
Department of Geology, The University of Iowa, Iowa City, Iowa 52242, U.S.A.

ABSTRACT

Biotite can act as a mineral catalyst that accelerates sillimanite-forming reactions in many high-grade pelites. In this process, biotite is replaced by sillimanite in one area while it is precipitated by local reactions in other areas of a rock. This mechanism develops because of the constraints imposed on material transport to and from growing sillimanite by minerals in the surrounding matrix. Textural evidence for biotite replacement is generally easily identified, but that for biotite-producing reactions is usually subtle. Failure to recognize the biotite-producing reactions can result in erroneous conclusions regarding the role of metasomatism in the formation of sillimanite. Models based on irreversible thermodynamics show that this type of reaction mechanism can develop where sillimanite grows under conditions that are isochemical at the hand-specimen scale.

Keywords: sillimanite, biotite, metamorphic differentiation, material transport, irreversible thermodynamics.

SOMMAIRE

La biotite peut catalyser les réactions qui produisent la sillimanite dans plusieurs pélites ayant un degré métamorphique élevé. Dans ce processus, la biotite est remplacée par la sillimanite à un endroit tandis qu'elle est formée suite à des réactions locales ailleurs dans la roche. Ce mécanisme a lieu à cause de contraintes imposées par les minéraux de la matrice sur le transfert de matière vers la sillimanite et en direction opposée. L'évidence texturale en faveur du remplacement de la biotite est claire, en général, mais celle qui signale la production de biotite est subtile. Des conclusions erronnées concernant le rôle de la métasomatose dans la formation de la sillimanite peuvent résulter si ces réactions ne sont pas repérées. Des modèles fondés sur la thermodynamique irréversible montrent que ce genre de réaction est important là où la sillimanite croît dans un milieu qui se comporte isochimiquement à l'échelle d'un seul échantillon.

(Traduit par la Rédaction)

Mots-clés: sillimanite, biotite, différenciation métamorphique, transfert de matière, thermodynamique irréversible.

INTRODUCTION

Many authors have made the observation that the nucleation and growth of sillimanite are commonly associated with biotite (*e.g.*, Chinner 1961, Kerrick 1990). In many metamorphic terranes, metapelites with small amounts of sillimanite contain needles of fibrolite within or fringing biotite. This observation suggests that biotite is the site with the lowest activation-energy for nucleation of sillimanite (Chinner 1961). Subsequent growth of sillimanite also appears to occur at the expense of biotite because textural relations clearly show that fibrolite replaced biotite. Good examples are shown in Kerrick (1990, Fig. 9.11). Some investigators (*e.g.*, Kerrick 1987, Kerrick & Woodsworth 1989, Vernon 1979) have used such textures to support the conclusion that a large-scale metasomatic process, such as leaching of base cations due to the influx of acid volatiles, is primarily responsible for the growth of sillimanite in the rocks they studied. Other authors (*e.g.*, Bailes & McRitchie 1978, Carmichael 1969, Yardley 1977) have proposed reaction mechanisms in which the local replacement of biotite by sillimanite is largely balanced by the growth of biotite in other areas of the rock. This process is essentially isochemical (except for the escape of volatiles) at the hand-specimen scale, and growth of sillimanite is attributed to the breakdown of lower-temperature mineral assemblages.

To choose between isochemical and metasomatic cases in rocks where sillimanite appears to grow at the expense of biotite, evidence for the presence or absence of local reactions that produce biotite must be found. Generally, the consumption of biotite by sillimanite can be easily documented because sillimanite directly replaces biotite. However, the production of biotite is usually difficult to detect because it grows at the expense of phases dispersed in a biotite-bearing matrix around the sillimanite. For example, consider the growth of sillimanite from kyanite by the reaction mechanism illustrated in Figure 1. In this case, the whole-rock reaction

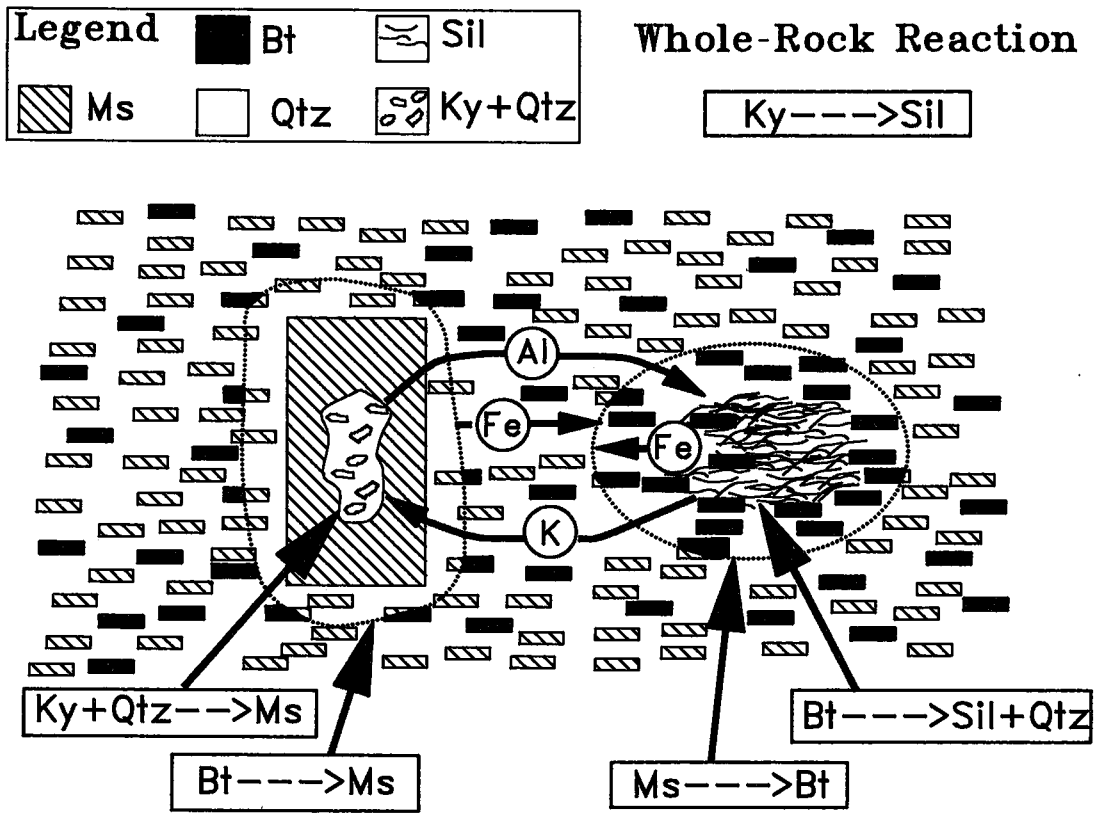

FIG. 1. Reaction mechanism using mica to catalyze the whole-rock reaction kyanite → sillimanite. Local reactions are given in rectangles at the bottom of the figure. Material transport of Fe, Al and K is shown by arrows drawn between reaction surfaces. The rectangular muscovite region around kyanite represents a muscovite pseudomorph after kyanite. The dotted line around the pseudomorph surrounds a biotite-free mantle formed by the breakdown of matrix biotite. The dotted line around the sillimanite segregation surrounds a muscovite-free mantle formed by the breakdown of matrix muscovite. Although significant amounts of biotite, muscovite and quartz take part in local reactions, there is no net gain or loss of any phases except for kyanite and sillimanite. Ky, Sil, Qtz, Ms and Bt stand for kyanite, sillimanite, quartz, muscovite and biotite, respectively (Kretz 1983).

is kyanite → sillimanite, caused by changing T and P of the rock. Although there are significant amounts of biotite and muscovite involved in the local reactions, there is no net change for either mica at the scale of a hand specimen. The same amounts are produced by local reactions in one part of the rock as are consumed by local reactions in other parts of the rock. In this instance, both biotite and muscovite are acting as mineral catalysts (*sensu* Carmichael 1969, p. 255) that accelerate the growth of sillimanite. Although there is considerable transport of material between reaction sites, the process will be isochemical at the hand-specimen scale in a medium-grained rock.

In Figure 1, the local reactions that lead to growth of sillimanite from biotite and to the replacement of kyanite with muscovite produce distinct textures that are easily recognized. The local reactions in the matrix produce subtle textures that are hard to detect. Failure to recognize the matrix reactions would result in the incorrect interpretation that the formation of sillimanite from kyanite was accompanied by the loss of Fe. This would lead to the erroneous conclusion that the growth of sillimanite was at least partially controlled by metasomatism, instead of P–T changes in an isochemical system. In most rocks, the easiest way to detect the matrix reactions would

be to look for a region of matrix around the sillimanite segregation that is muscovite-free and a region of matrix around the kyanite pseudomorph that is biotite-free. Tracings of thin sections and photomicrographs showing muscovite-free regions produced by reactions in the matrix around sillimanite segregations are illustrated in Foster (1977, Figs. 4, 5). A camera lucida drawing that shows a biotite-free mantle adjacent to partially replaced kyanite is shown by Hietanen (1963, Fig. 6).

Mass-balance studies (Foster 1977) and simulations based on principles of irreversible thermodynamics (Foster 1981, 1982a, b, 1983, 1986, 1990b) indicate that it is common for biotite to act as a catalyst for the growth of sillimanite. Consequently, caution must be used in proposals of reaction mechanisms for sillimanite growth in micaceous rocks. Mass-balance techniques can sometimes help to evaluate reaction mechanisms of this type, but they can only be of significant value where the composition of the original protolith is known or the amount of open-system behavior can be approximated. An approach based on irreversible thermodynamics is generally more useful because it predicts textural features that can be compared with those in the rocks, allowing hypotheses to be tested. This method also provides insight into the fundamental controls on reaction mechanisms. For example, it suggests that the type

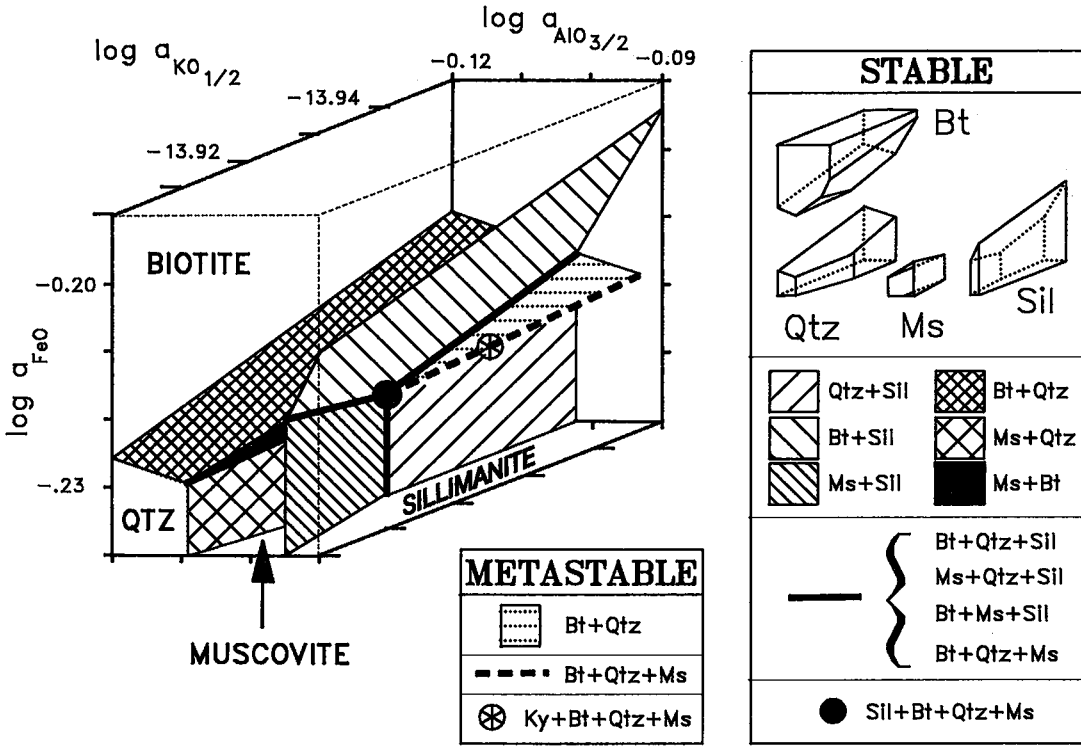

FIG. 2. Activity diagram drawn for conditions of 627°C and 6 kbar showing stability fields of biotite, quartz, muscovite and sillimanite as a function of the activities of FeO, $AlO_{3/2}$, and $KO_{1/2}$. Water is present everywhere on the diagram. The choices of components and standard states are explained in the text. There are four types of stable features shown on the diagram: i) four volumes that represent conditions where one mineral in equilibrium with water is the most stable assemblage (shown in an exploded view in the legend), ii) six divariant surfaces that represent conditions where two minerals plus water constitute the most stable equilibrium-assemblage, iii) four univariant lines that represent conditions where three minerals plus water constitute the most stable assemblage, and iv) one invariant point where Sil + Bt + Qtz + Ms plus water is the most stable assemblage. There are also three features shown on the diagram that represent the conditions of metastable equilibria within the sillimanite stability-volume: i) an invariant point representing the metastable assemblage Ky + Bt + Qtz + Ms plus water, ii) the metastable extension of the univariant line representing the assemblage Bt + Qtz + Ms plus water, and iii) the metastable extension of the divariant surface representing the assemblage Bt + Qtz plus water.

of process illustrated in Figure 1 develops because of the constraints that local equilibrium imposes on gradients in chemical potentials that drive material transport.

Reaction Mechanisms and Material Transport

The nucleation and growth of sillimanite require the sillimanite-forming reaction to be overstepped and the pre-existing mineral assemblage to be metastable. Initially, just after sillimanite has nucleated, the rock will react under disequilibrium conditions. As the reaction progresses, conditions will generally move toward those of equilibrium. In most cases, local equilibrium will be established with nearby mineral phases (Fisher 1978, Walther & Wood 1986, Knapp 1989). Once local equilibrium has been established, the stoichiometry of the reaction at the site of sillimanite growth is largely determined by the constraints on material transport imposed by the distribution of metastable mineral assemblages surrounding the site of nucleation (Foster 1990a).

The constraints on material transport produced by the nucleation and growth of sillimanite (Sil) in the commonly observed matrix assemblage muscovite (Ms) + biotite (Bt) + quartz (Qtz) + water (Wa) can be investigated using the activity diagram shown in Figure 2. It has been drawn for water-saturated conditions corresponding to 627°C, 6 kbar using the data of Helgeson *et al.* (1978). The equilibria represented by divariant surfaces on this diagram have been written to conserve silica, conforming to a silica-fixed frame of reference (Brady 1975), which is equivalent to an inert marker frame of reference in quartz-bearing rocks under a hydrostatic stress (Foster 1981, p. 265). The activities of K, Al and Fe have been expressed as those of the oxides, with the standard state chosen so that $KO_{1/2}$ has unit activity when the system is saturated with potassium oxide at the T and P of interest. Similarly, $AlO_{3/2}$ and FeO have unit activity when the system is saturated with corundum and ferrous oxide, respectively, at the T and P of interest. This convention has been chosen for convenience, to avoid complications involving the uncertainties in speciation, particularly of Al, in the grain-boundary fluid phase at metamorphic temperatures and pressures (Walther 1986, Woodland & Walther 1987, Eugster & Baumgartner 1987). If one can specify a dominant species at the T and P of interest, the diagrams can be easily converted to aqueous species by using equilibrium constants for reactions such as $KO_{1/2} + HCl \rightarrow KCl + 0.5\ H_2O$. In order for sillimanite to nucleate in a rock containing muscovite, biotite, quartz and water, conditions must lie along the metastable extension of the Bt + Qtz + Ms univariant line into the stability volume of sillimanite, shown as a dashed line in Figure 2. Once nucleation has taken place and local equilibrium has been established between newly nucleated fibrolite and the surrounding minerals, the local chemical potentials are fixed at the values of the invariant point Sil + Bt + Qtz + Ms in Figure 2. However, the chemical potentials in the matrix some distance away from the sillimanite, which has not been affected by the sillimanite-forming reaction, still have values that lie on the metastable extension of the Bt + Qtz + Ms line. This difference in chemical potentials between the region in local equilibrium with sillimanite and the rest of the rock produce gradients in chemical potential that drive material transport to and from the site of sillimanite nucleation. Because the chemical potentials in the matrix are constrained to lie along the metastable extension of the Bt + Qtz + Ms line, the chemical potentials of FeO and $AlO_{3/2}$ are higher in the matrix than at the site of sillimanite nucleation, whereas the chemical potential of $KO_{1/2}$ will be lower in the matrix than at the site of sillimanite nucleation. This causes Fe and Al species to diffuse through the matrix toward the sillimanite, and K to diffuse through the matrix away from the sillimanite. The transport of material will cause sillimanite to react with nearby matrix minerals and the grain-boundary phase to maintain local equilibrium. This reaction will replace muscovite with sillimanite + biotite ± quartz. The stoichiometry of the reaction is controlled by the composition of the minerals and the fluxes of material into and out of the volume of the rock where the reaction takes place (Fisher 1975, 1977).

As shown in the appendix, these constraints are sufficient to allow calculation of the reaction among the matrix minerals and the grain-boundary phase that is required to produce one mole of sillimanite:

$$0.21\ FeO + 0.72\ AlO_{3/2} + 0.45\ Ms \rightarrow 1.0\ Sil + 0.07\ Bt + 0.14\ Qtz + 0.38\ Wa + 0.38 KO_{1/2} \quad (1)$$

The oxides listed in the reaction are the amounts of Fe, K and Al that are supplied through the grain-boundary phase owing to gradients in chemical potentials in the matrix. SiO_2 and H_2O are balanced by quartz in the matrix and water along the grain boundaries, respectively. These two phases are usually present everywhere in the rock, preventing development of gradients in chemical potentials in SiO_2 and H_2O that would drive diffusive transport of these components.

Growth of Sillimanite Nodules

The texture produced by reaction (1) is largely dependent upon the number of nuclei that form in the rock before significant growth of sillimanite takes place. Rocks with few nuclei will produce large isolated segregations or porphyroblasts, whereas rocks with many nuclei will produce small, abundant sillimanite crystals or fibrolite segregations. The morphology of the textures produced by these two cases generally begins to diverge when the diameter of the sillimanite porphyroblast or fibrolite cluster exceeds the size of mica crystals in the matrix. If only a few nuclei form before significant growth of sillimanite takes place, reaction (1) will consume all of the muscovite in the immediate vicinity of the sillimanite, producing a muscovite-free mantle [designated as (Ms), for muscovite-absent] around the sillimanite. The values of the chemical potentials inside of the (Ms) mantle are no longer constrained by local equilibrium with muscovite, and the chemical potentials are free to move onto the metastable extension of the Bt + Qtz divariant surface, shown as a dotted surface in Figure 2. Values of the chemical potentials at the inner margin of the (Ms) mantle are free to move along the Bt + Qtz + Sil univariant line, shown as a heavy solid line located to the upper right of the Sil + Bt + Qtz + Ms invariant point in Figure 2. Conditions at the outer margin of the (Ms) mantle are still constrained by the assemblage muscovite + biotite + quartz + water, and must lie along the metastable (dashed) part of the Bt + Qtz + Ms univariant line in Figure 2. If local equilibrium is to be maintained at the inner boundary of the (Ms) mantle, the gradients in chemical potentials within the mantle must change so that the fluxes can be balanced by a reaction among the phases sillimanite, biotite, quartz and water. The values of the chemical potentials in the (Ms) mantle also must lie on the metastable Bt + Qtz surface shown on Figure 2. These constraints on the chemical potential gradients transporting components to and from the reaction site allow calculation (see Appendix) of the reaction for the portion of the segregation enclosed by the (Ms) mantle:

$$1.93\ AlO_{3/2} + 0.07\ Bt + 0.79\ Qtz \rightarrow 1.0\ Sil + 0.07\ KO_{1/2} + 0.21\ FeO + 0.07\ Wa \quad (2)$$

The Al for reaction (2) is supplied by diffusion through the (Ms) mantle, whereas the K and Fe produced by this reaction are removed by diffusion through the (Ms) mantle.

Reaction (2) will consume either all of the biotite or all of the quartz in the vicinity of the growing sillimanite, and leave a region composed entirely of quartz or entirely of biotite adjacent to the sillimanite. If the biotite is consumed first, then the reaction at the sillimanite–quartz boundary inside the biotite-free, muscovite-free (MsBt) mantle will be (see Appendix):

$$2\ AlO_{3/2} + 1.0\ Qtz \rightarrow 1.0\ Sil \quad (3)$$

If reaction (2) consumes all the quartz in the vicinity of the growing sillimanite, then the reaction in the portion of the segregation surrounded by the muscovite-free, quartz-free (MsQtz) mantle will be (see Appendix):

$$1.68\ AlO_{3/2} + 0.04\ SiO_2 + 0.32\ Bt \rightarrow 1.0\ Sil + 0.32\ KO_{1/2} + 0.96\ FeO + 0.32\ Wa \quad (4)$$

Mantle reactions

Reactions (1) + (2) + (3) or (1) + (2) + (4) operate simultaneously in a single segregation and produce a sequence of mantles around the growing sillimanite: an outer muscovite-free mantle (Ms) composed of biotite + quartz, and either a (MsQtz) inner mantle composed of biotite or a (MsBt) inner mantle composed entirely of quartz. The three local reactions that take place inside of a segregation can be calculated from reactions (1) through (4) (see Appendix). For a segregation with an (MsBt) inner mantle, the local reactions are:

$$0.42\ FeO + 0.45\ Ms \rightarrow 0.14\ Bt + 0.93\ Qtz + 0.31\ KO_{1/2} + 1.21\ AlO_{3/2} + 0.31\ Wa \quad (5)$$

at the (Ms) mantle – matrix boundary,

$$0.07\ Bt \rightarrow 0.21\ Qtz + 0.07\ KO_{1/2} + 0.21\ FeO + 0.07\ Wa + 0.07\ AlO_{3/2} \quad (6)$$

at the (Ms) mantle – (MsBt) mantle boundary, and reaction (3) at the (MsBt) mantle – sillimanite core interface. For a segregation with an (MsQtz) inner mantle, the local reactions are: reaction (5) at the (Ms) mantle-matrix boundary,

$$0.25\ KO_{1/2} + 0.25\ AlO_{3/2} + 0.75\ FeO + 0.25\ Wa + 0.79\ Qtz \rightarrow 0.25\ Bt + 0.04\ SiO_2 \quad (7)$$

at the (Ms) mantle – (MsQtz) mantle boundary, and reaction (4) at the boundary between the sillimanite core and the (MsQtz) mantle that surrounds it.

Segregation morphology

The mineral modes and relative sizes of the mantles can be calculated from the modes of the

matrix and the appropriate combinations of reactions (3), (4), (5), (6), and (7) (see Appendix). The morphology, mineral modes, component sources and sinks, and component fluxes calculated for a segregation that grew when sillimanite nucleated in a matrix that contained 20% biotite, 30% muscovite and 50% quartz are shown in Figure 3. Typical examples of sillimanite segrega-

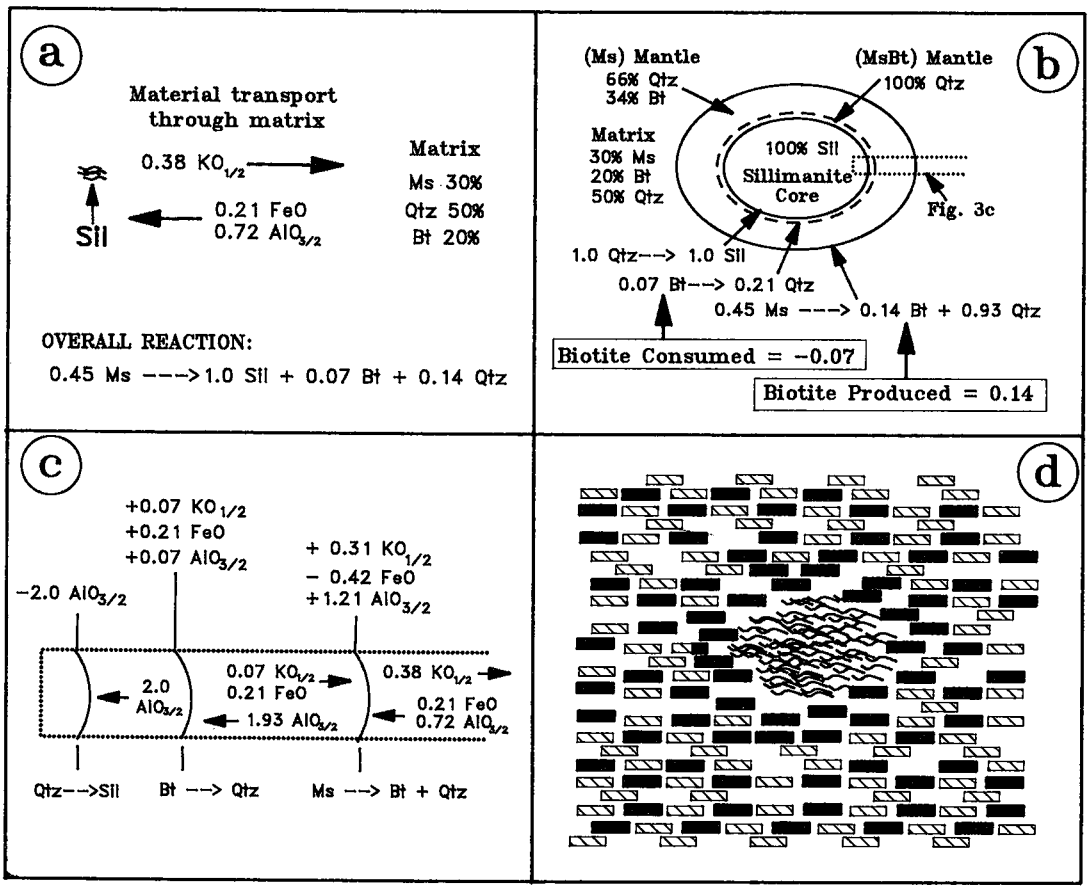

FIG. 3. Calculated reaction-model for nodular segregations of sillimanite in muscovite-bearing rocks. a) Starting configuration: sillimanite nucleates in a Ms + Bt + Qtz matrix. The overall reaction is reaction (1). Material transport through the matrix removes K produced by the overall reaction and supplies Fe and Al consumed by the overall reaction. b) Stoichiometry of minerals involved in local reactions, mineral modes, and segregation morphology that develops from the starting configuration. Note that more biotite is produced at the margin of the segregation than is consumed in the interior of the segregation, so that there is a net production of biotite equal to 0.07 moles of biotite per mole of sillimanite growth. The dotted line gives the location of the area enlarged to make Figure 3c. c) An enlarged section of Figure 3b showing the sources, sinks, and transport of components among reaction sites. The sillimanite core is on the left, the matrix is on the right, and the (MsBt) and (Ms) mantles are in the middle. Each vertically oriented curved line represents a reaction surface for the local reaction listed beneath it. The amounts of each component produced (+) or consumed (-) by a local reaction are listed above the curved line representing the reaction surface. The amounts and direction of material transport are shown by numbers with arrows between the reaction interfaces. The amounts shown are normalized to one mole of sillimanite produced in the core of the segregation. d) Simulated texture produced from reaction model in Figure 3b. Biotite is black, muscovite has a diagonal pattern, wavy lines are sillimanite, and uncolored areas are polycrystalline quartz. The diameter of the sillimanite core is typically a few mm in most pelites, but it can be larger than several cm in rare instances. The biotite-rich mantle around sillimanite is subtle because the new biotite in the mantle is similar to the more abundant grains of matrix biotite in the mantle.

tions with these mantles are illustrated in Foster (1977, Figs. 4, 5; 1982a, Fig. 6) and Bailes & McRitchie (1978, Figs. 23, 25 and 27). The dark rim at the edge of the fibrolite segregations in the illustrations cited consists of a network of sillimanite fibers in quartz that represent the inner margin of the quartz (MsBt) mantle shown in Figure 3b. Because the width of the (MsBt) mantle in many pelites is less than the length of biotite crystals in the matrix, it is common for a (MsQtz) mantle to develop where there is a local increase in the mode of biotite due to the presence of a few closely spaced biotite flakes. This will result in the growth of sillimanite directly on biotite rather than on quartz. In many rocks, it is common for both types of inner mantles to be present, so that sillimanite replaces both biotite and quartz, depending upon variations in the local mineral modes of the matrix where sillimanite nucleated.

An important feature of the reaction mechanism shown in Figure 3 is that biotite is acting as a mineral catalyst by dissolving in one area and precipitating in another (Carmichael 1969, p. 255). Reactions of this type can create a problem in methods that use changes in the modal abundances of minerals in the bulk rock to infer the P-T-*X* path followed during metamorphism. Several studies have shown this approach to be a powerful tool in the interpretation of the history of metamorphic rocks (*e.g.*, Thompson 1982, Spear 1988, Schneiderman 1990), but care must be taken to correctly identify the net changes of mineral modes in the rock as a whole. This commonly is difficult because most reactions proceed by mechanisms that involve mineral catalysts. In many cases, the resulting textures include subtle mantles around porphyroblasts, segregations, and pseudomorphs that are easily misinterpreted because the mantles are texturally similar to the matrix they replaced. In addition, many minerals will be present as two generations: "old" crystals that were present in the matrix before the mantle formed, and "new" crystals formed by the reaction that created the mantle. Typically, most of the minerals in a mantle are of the "old" generation, giving the mantle many characteristics that are similar to the matrix from which it formed. In the example illustrated in Figure 3, half of the biotite produced by reaction (5) at the outer edge of the (Ms) mantle is consumed by reaction (6) at the inner edge of the (Ms) mantle (Fig. 3b). Recognition of the amount of biotite produced at the (Ms) mantle – matrix boundary commonly is difficult because almost two thirds of the biotite in the (Ms) mantle is "old" biotite that was present in the matrix before sillimanite began to grow, and the "new" biotite is commonly texturally similar to it (Fig. 3d; Foster 1977, Fig. 5; Foster 1982a, Fig. 6; Foster 1986, Fig. 1). Failure to realize that the reaction at the (Ms) mantle – matrix boundary is an important part of the mechanism of sillimanite growth might cause an investigator to conclude that the reaction for the rock as a whole was *consuming* 0.07 moles of biotite per mole of sillimanite growth rather than *producing* 0.07 moles. This error would suggest that the processes responsible for sillimanite growth involved removal of Fe instead of addition of Fe.

Growth of Dispersed Sillimanite

Another growth morphology of sillimanite is that in which many sillimanite nuclei form in the rock before much growth takes place. This distributes the sites of sillimanite growth throughout the rock, and produces many small clusters of fibrolite or small prisms of sillimanite. The constraints on material transport during the growth of sillimanite in each enclave where it nucleated are the same as those discussed in the previous section. However, because the size of the sillimanite segregation is about the same as the size of mica flakes in the rock, the composition of the matrix being consumed by the sillimanite-forming reaction is not homogeneous at the scale of the segregation. Consider the situation shown in Figure 4a, where sillimanite has nucleated along a biotite–quartz grain boundary and begins to grow. The material transport to the sillimanite along immediately adjacent grain-boundaries will be driven by gradients in chemical potential that are in local equilibrium with quartz and biotite. However, as in the case where few nuclei form, material transport through the matrix surrounding the nucleus will be driven by gradients in chemical potential that are in local equilibrium with muscovite + biotite + quartz + water because all of these phases will be present within a few crystal diameters of the sillimanite nucleus. This means that the sum of the local reactions at the biotite + quartz + sillimanite interface must be reaction (2), and the local reactions at the surface where the first muscovite is encountered must sum to reaction (5).

The site where reaction (2) is taking place is not compositionally homogeneous at the scale of the reaction interface. One side of the sillimanite is 100% biotite, and the other side is 100% quartz. This causes reaction (2) to split into two local reactions, one that forms sillimanite from biotite, and the other that forms sillimanite from quartz:

$$0.35\ AlO_{3/2} + 0.07\ Bt \rightarrow 0.21\ Sil + 0.21\ FeO + 0.07\ KO_{1/2} + 0.07\ Wa \qquad (8)$$

and

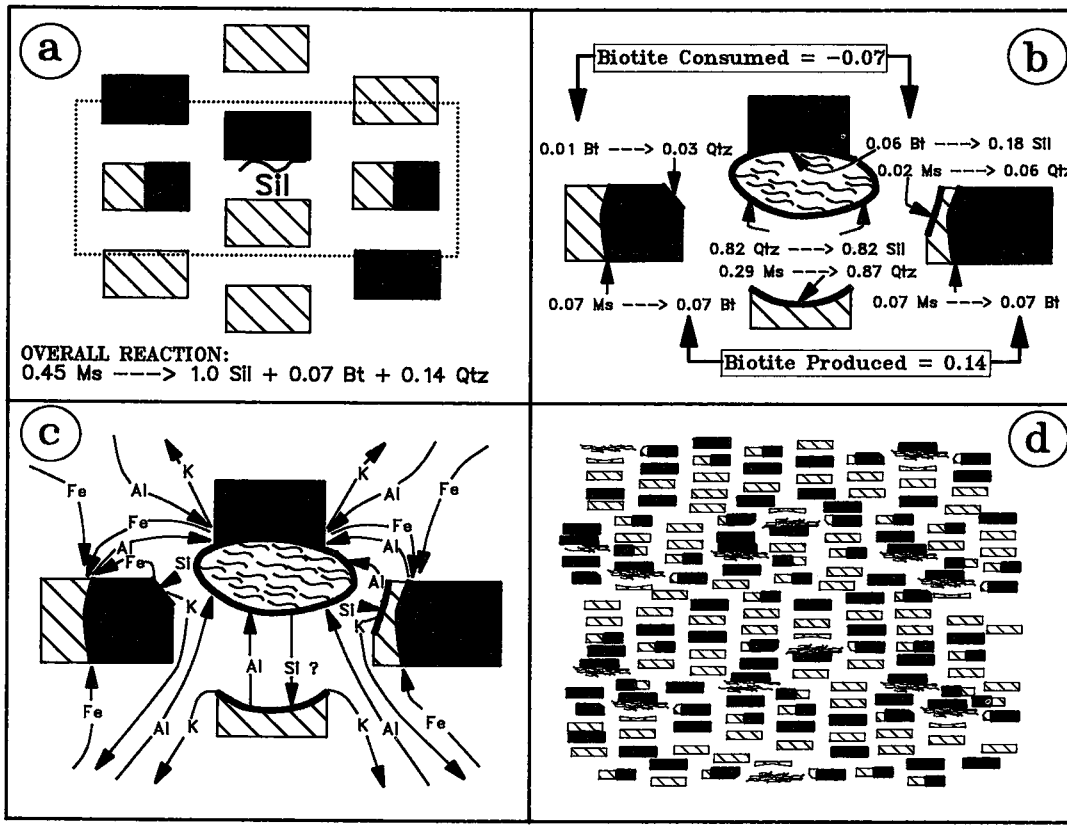

FIG. 4. Calculated reaction-model for disseminated sillimanite segregations in muscovite-bearing rocks. Biotite is black, muscovite has diagonal pattern, sillimanite is represented by wavy lines, and uncolored areas are polycrystalline quartz. The width of panels a, b, and c in this figure is much smaller than equivalents on Figure 3. The width of panel d in this figure is about the same as in Figure 3. a) Starting configuration: sillimanite nucleates adjacent to biotite. The overall reaction is constrained to be reaction (1) by limits on material transport through the matrix. The minerals involved in the overall reaction are given at the bottom of the figure. The dotted rectangle is the area enlarged for Figure 4b and 4c. b) Local reactions and textures that develop from the starting configuration. Sillimanite replaces biotite, but the sum of the local reactions produces 0.07 moles of biotite per mole of sillimanite growth. c) Paths of material transport. Oxide portions of the component labels have been omitted. Si means transport of SiO_2 may be taking place owing to local stress-gradients caused by the volume increase in local reactions where sillimanite replaces quartz. d) Schematic texture produced by the reaction model in Figure 4b. Mica flakes in a typical pelite with this texture are about 0.5 mm across. Compare with Figure 3d.

$$1.58\ AlO_{3/2} + 0.79\ Qtz \rightarrow 0.79\ Sil \qquad (9)$$

Reaction (8) essentially conserves volume, whereas reaction (9) involves a substantial increase in volume. Many investigators (*e.g.*, Chinner 1961, Fig. B; Kerrick 1990, Fig. 9.11) have shown illustrations of undeformed grains of biotite intergrown with sillimanite, which suggests that volume is conserved where biotite is replaced by sillimanite. The case is less clear regarding quartz replacement by sillimanite, but most textures do not appear to support large changes in volume in this reaction either (*e.g.*, Vernon 1979, Figs. 2f, 2g). Local gradients in stress set up by volume increases due to reaction (9) may result in chemical potential gradients that transport silica away from the site of volume increase. This results in more quartz dissolution in the reaction Qtz → Sil than is predicted by reaction (9).

The site where reaction (5) is taking place also is not compositionally homogeneous because the size of the sillimanite is small compared to the grain

size of the matrix. The reaction will be partitioned into local reactions that replace muscovite with quartz and muscovite with biotite:

$$0.31\ \text{Ms} \rightarrow 0.93\ \text{Qtz} + 0.31\ \text{KO}_{1/2} + 0.93\ \text{AlO}_{3/2} + 0.31\ \text{Wa} \quad (10)$$

and

$$0.42\ \text{FeO} + 0.14\ \text{Ms} \rightarrow 0.14\ \text{Bt} + 0.28\ \text{AlO}_{3/2} \quad (11)$$

Figure 4 shows the local reactions, morphology and paths of material transport produced by the nucleation and growth of a small amount of sillimanite in a rock where the grain size of the matrix is approximately the same as that of the sillimanite segregations. In Figure 4b, reactions (8), (9), (10) and (11) have been partitioned among the sites of local reaction based upon their proximity to the point of sillimanite growth. The paths of material transport shown in Figure 4c are based upon the chemical potential gradients permitted by local equilibrium and the sources and sinks of the local reactions shown in Figure 4b. As in the case of the sillimanite nodule, biotite is acting as a catalyst in the growth of disseminated sillimanite (Fig. 4b), so that the observation that biotite is being replaced by sillimanite may lead to the erroneous conclusion that biotite is being consumed during the overall reaction in the rock, when in fact it is being produced. As shown in Figure 4d, this sort of reaction is usually extremely difficult to evaluate, because matrix muscovite is only partially dissolved, and no distinct (Ms) mantle forms around the sillimanite.

Closed Versus Open Systems

In the examples discussed above, the sillimanite segregation occurs in an open system, being linked by diffusion through the matrix to an unspecified source or sink that provides or consumes the constituents that must be transported through the matrix to balance reaction (1). There are two possible locations for these sources and sinks: i) they can be outside of a typical hand specimen, so that the system is open to many components at the scale of a hand specimen or, ii) they can be located within a typical hand specimen so that a hand specimen is closed to all components (except perhaps minor amounts of volatiles). In the first case, diffusion through the matrix transports constituents to and from nearby fluid-infiltration pathways that are capable of transporting constituents over distances larger than a hand specimen. In this situation, metasomatism due to fluid flow is an important control of metamorphism. In the second case, diffusional transport of constituents between domains with local reactions that balance each other occurs within a hand specimen. In this situation, metasomatism beyond the scale of a hand specimen is unimportant, and the metamorphism is controlled primarily by changes in temperature and pressure.

The distribution of reactants in the rock while sillimanite grows plays an important role in the textures that develop. Two examples are considered below: one is the situation where the mineral being consumed to form the sillimanite is present as porphyroblasts in the rock; the other is a situation where the mineral is disseminated throughout the matrix. In one case, the whole-rock reaction is completely isochemical, and in the other, it is isochemical except for the escape of water. In both cases, the material-transport constraints provided by the mineral assemblages around the nucleation sites of sillimanite cause reactions that produce good textural evidence for biotite consumption and only subtle evidence for biotite growth. Overlooking the biotite-producing reactions would lead to the erroneous conclusion that the formation of sillimanite was caused by base-cation leaching (or hydrogen metasomatism), where in fact both reactions are the result of thermal effects in a system closed to all components but water.

Kyanite Breakdown

A good example of the situation where sillimanite grows at the expense of a porphyroblast mineral is the breakdown of kyanite to form sillimanite as the result of isobaric heating at six kilobars. At this pressure, sillimanite is the stable polymorph of Al_2SiO_5 at temperatures above 617°C, and kyanite is stable below this temperature. If the temperature in the rock exceeds 617°C, kyanite is metastable with respect to sillimanite, but no reaction takes place until the first nuclei of sillimanite form in the rock. Nucleation of sillimanite requires the equilibrium temperature to be overstepped to an unknown extent. For purposes of discussion, it is assumed that nucleation and growth of fibrolite on biotite take place when the kyanite = sillimanite equilibrium temperature has been exceeded by 10°C. This corresponds to the T and P at which the activity diagram in Figure 2 was calculated. The conditions in the rock just after sillimanite has nucleated are shown in Figure 5a. Prior to sillimanite nucleation, the rock consisted of kyanite porphyroblasts set in a uniform matrix composed of 50% quartz, 30% muscovite, 20% biotite and a water-rich grain-boundary phase. As noted by Chinner (1961), the most favorable site for fibrolite nucleation in many rocks appears to

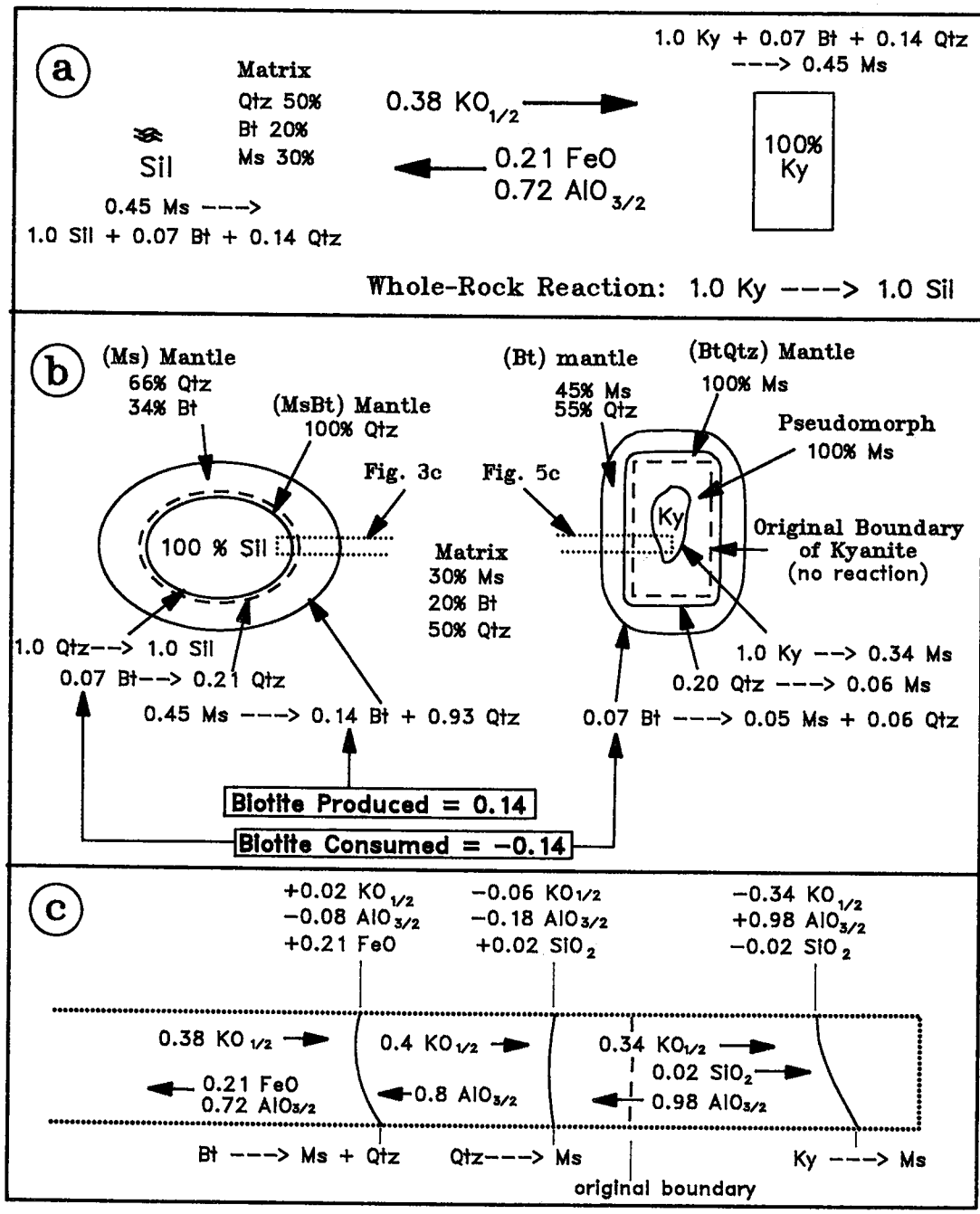

FIG. 5. Calculated reaction-model for sillimanite segregations that grow in a rock with kyanite pseudomorphs. a) Starting configuration showing the minerals involved in overall reactions near sillimanite and kyanite, the material transport between kyanite and sillimanite, and the whole-rock reaction. b) Local reactions, mineral modes and segregation morphology. The amount of biotite consumed near sillimanite and kyanite is exactly balanced by the biotite produced from muscovite breakdown at the edge of the sillimanite segregation. Dotted lines show areas enlarged in Figures 3c and 5c to illustrate sources, sinks and material transport. c) Material transport, sources and sinks along a profile from the kyanite remnant (right) to the matrix (left). The original boundary of the kyanite porphyroblast is shown by a dashed line within the pseudomorph. Other notation is the same as in Figure 3c.

be biotite. Therefore, in this simulation, fibrolite has been allowed to nucleate on a flake of biotite in the matrix some distance from a kyanite porphyroblast. When the fibrolite has established local equilibrium with the surrounding matrix minerals, it will lie at conditions given by the stable Sil + Bt + Qtz + Ms invariant point, shown as a filled circle in Figure 2. Conditions in the rock near the kyanite porphyroblast are given by the location of the metastable Ky + Bt + Qtz + Ms invariant point, shown as a spoked circle in Figure 2. The values of the log of the activities of $AlO_{3/2}$, $KO_{1/2}$, and FeO at the Ky + Bt + Qtz + Ms invariant point are -0.0995, -13.931, and -0.2226, respectively; the values at the Sil + Bt + Qtz + Ms invariant point are -0.1026, -13.922 and -0.2246, respectively. Thus, K should be transported from the vicinity of sillimanite to kyanite, whereas the transport of Fe and Al should be in the opposite direction, from kyanite to sillimanite. The removal of Al from the vicinity of kyanite causes kyanite to dissolve to maintain local equilibrium with quartz, whereas the addition of Al to the local environment around sillimanite results in the precipitation of sillimanite to maintain local equilibrium with quartz. The values of the activities of components in the matrix between kyanite and sillimanite are constrained by the assemblage muscovite + biotite + quartz + water to have values given by the metastable portion of the Bt + Qtz + Ms univariant line between the two invariant points in Figure 2. The relative values of the gradients in chemical potentials in the matrix around the two aluminosilicates thus are fixed at the same values, so that the diffusive transport to and from the sillimanite will exactly balance the transport to and from the kyanite. For values of the diffusion coefficients given by Foster (1981), this means that 0.21 moles of FeO and 0.72 moles of $AlO_{3/2}$ will be transported through the matrix from kyanite to sillimanite and 0.38 moles of $KO_{1/2}$ will be transported from sillimanite to kyanite, when one mole of sillimanite has grown in the rock. The only reaction among sillimanite and the matrix minerals that can produce 0.38 moles of K while consuming 0.21 moles of Fe and 0.72 moles of Al is reaction (1). The only reaction between kyanite and the matrix minerals that can consume 0.38 moles of K while producing 0.21 moles of Fe and 0.72 moles of Al is:

$$0.38\ KO_{1/2} + 1.0\ Ky + 0.07\ Bi + 0.14\ Qtz + 0.38\ Wa \rightarrow 0.45\ Ms + 0.21\ FeO + 0.72\ AlO_{3/2} \quad (12)$$

If only a few nuclei form before appreciable growth takes place, reaction (1) produces a sillimanite segregation with (Ms) and (MsBt) mantles, as discussed above in the section on sillimanite nodules. Reaction (12) replaces kyanite with muscovite and also consumes biotite and quartz adjacent to the porphyroblast. For the matrix composition given in Figure 5a, biotite will be consumed before the quartz, forming a biotite-free (Bt) mantle that progresses out into the matrix around the kyanite. If this happens, the material transport to and from the kyanite through the muscovite + quartz mantle is no longer constrained by the Gibbs–Duhem equation for biotite. The only reaction among the minerals in the portion of the kyanite pseudomorph surrounded by the (Bt) mantle that can satisfy the constraints on material transport imposed by the diffusion-coefficient ratios of Foster (1981) and chemical potential gradients in local equilibrium with the assemblage muscovite + quartz is:

$$0.4\ KO_{1/2} + 0.4\ Wa + 0.20\ Qtz + 1.0\ Ky \rightarrow 0.4\ Ms + 0.8\ AlO_{3/2} \quad (13)$$

Subtracting reaction (13) from reaction (12) gives the reaction at the (Bt) mantle - matrix boundary:

$$0.08\ AlO_{3/2} + 0.07\ Bt \rightarrow 0.05\ Ms + 0.06\ Qtz + 0.02\ KO_{1/2} + 0.21\ FeO \quad (14)$$

Application of the approach used to calculate modes in the (Ms) mantle of the sillimanite segregation (see Appendix) allows the mineral modes in the (Bt) mantle of the kyanite pseudomorph to be computed from reaction (14). They are 45% Ms and 55% Qtz.

Reaction (13) represents the reaction taking place in the volume of rock surrounded by the (Bt) mantle. This reaction is actually the sum of two local reactions, one that advances out into the matrix from the original boundary of the kyanite, replacing quartz with muscovite, and another that advances into the porphyroblast, replacing kyanite with muscovite. The stoichiometry of the reaction that advances into the porphyroblast can be calculated by solving for the reaction among muscovite, kyanite and water that will produce and consume constituents in the correct amounts to be transported away through the muscovite pseudomorph under conditions of local equilibrium. Application of the same diffusion coefficients used to calculate reaction (4) (see Appendix) gives the reaction at the pseudomorph–kyanite boundary:

$$0.02\ SiO_2 + 0.34\ KO_{1/2} + 0.34\ Wa + 1.0\ Ky \rightarrow 0.34\ Ms + 0.98\ AlO_{3/2} \quad (15)$$

Note that reaction (15) is insensitive to the value chosen for the silica coefficient ratio if the values

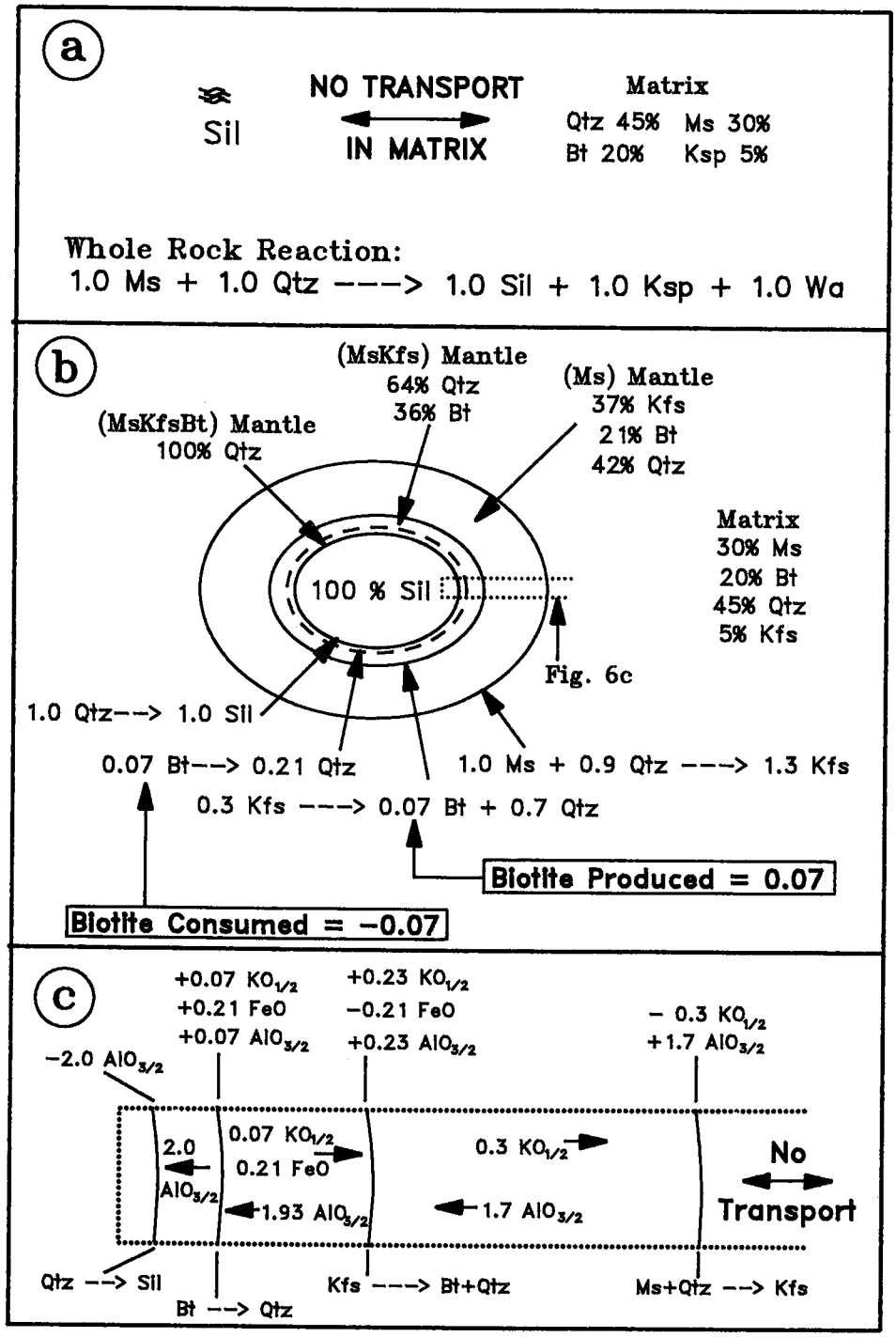
a
Sil
NO TRANSPORT
IN MATRIX
Matrix
Qtz 45% Ms 30%
Bt 20% Ksp 5%
Whole Rock Reaction:
1.0 Ms + 1.0 Qtz ---> 1.0 Sil + 1.0 Ksp + 1.0 Wa
b
(MsKfs) Mantle
64% Qtz
36% Bt
(Ms) Mantle
37% Kfs
21% Bt
42% Qtz
(MsKfsBt) Mantle
100% Qtz
Matrix
30% Ms
20% Bt
45% Qtz
5% Kfs
100 % Sil
Fig. 6c
1.0 Qtz--> 1.0 Sil
0.07 Bt--> 0.21 Qtz
1.0 Ms + 0.9 Qtz ---> 1.3 Kfs
0.3 Kfs ---> 0.07 Bt + 0.7 Qtz
Biotite Produced = 0.07
Biotite Consumed = -0.07
c
+0.07 KO1/2
+0.21 FeO
+0.07 AlO3/2
+0.23 KO1/2
-0.21 FeO
+0.23 AlO3/2
- 0.3 KO1/2
+1.7 AlO3/2
-2.0 AlO3/2
2.0
AlO3/2
0.07 KO1/2
0.21 FeO
1.93 AlO3/2
0.3 KO1/2
1.7 AlO3/2
No
Transport
Qtz --> Sil
Bt --> Qtz
Kfs ---> Bt+Qtz
Ms+Qtz --> Kfs

of Foster (1981) are used for the other coefficient ratios (Foster 1990a, Fig. 6).

The reaction at the pseudomorph – (Bt) mantle boundary can be found by subtracting reaction (15) from reaction (13):

$$0.06\ KO_{1/2} + 0.18\ AlO_{3/2} + 0.06\ Wa + 0.20\ Qtz \rightarrow 0.06\ Ms + 0.02\ SiO_2 \quad (16)$$

Reaction (16) produces a small amount of muscovite pseudomorph that is actually beyond the original boundary of the kyanite crystal. Because the composition is the same on both sides of the boundary, the original position of the kyanite–matrix boundary could only be identified if the muscovite produced by reaction (16) was texturally different from that produced by reaction (15) or if there was some sort of inert marker such as graphite concentrated along the boundary before kyanite began to dissolve.

The morphology, mineral modes and local reactions for the sillimanite segregation and kyanite pseudomorph are shown in Figure 5b. The component sources, sinks, and relative fluxes in the regions around the kyanite and sillimanite are shown in Figures 5c and 3c, respectively. Figure 5b shows that there is no net production of biotite in the rock as a whole, even though the volume of biotite that is consumed and reprecipitated at different locations is equal to about half of the volume of sillimanite that grows in the rock. The only local reaction involving biotite that can be easily identified in thin section tends to be the replacement of biotite by sillimanite + quartz at the inner margin of the sillimanite segregation. The consumption of biotite in the matrix around the kyanite pseudomorph is commonly difficult to recognize because the change in mode is subtle compared to that present at the (Bt) mantle – pseudomorph boundary. Consequently, this reaction is easily overlooked. Similarly, the biotite-producing reaction at the outer margin of the sillimanite segregation may not be recognized because it is marked by a subtle change in mode. This is particularly true in medium- and coarse-grained rocks, where the width of the (Ms) mantle is less than a few times the size of mica flakes in the matrix. In this situation, a more reliable way to detect the biotite-producing reaction is to look for muscovite depletion in the matrix around the sillimanite. The (Ms) mantles also can be detected in hand specimens because the slightly higher biotite mode in the (Ms) mantle causes the region immediately adjacent to the sillimanite cores to be slightly darker than the matrix away from the sillimanite. The only reliable way to quantitatively estimate the amount of biotite produced or consumed by local reactions in such rocks is by careful textural analysis and extensive point-counting with small intervals.

Muscovite Breakdown

Complete identification of all local reactions in a rock is even more difficult if the mineral consumed by the overall reaction is dispersed throughout the matrix. In this case, little evidence of the original mineral is left in the rock once the reaction is complete. At first glance, the textures present in this type of rock commonly suggest that it has been an open system affected by significant amounts of metasomatism, even though the actual process was largely closed at the scale of a hand specimen. An example of this type of reaction is the formation of sillimanite nodules during the breakdown of muscovite. Many nodular sillimanite rocks found in low-pressure upper-amphibolite-facies terranes may have originated by this mechanism. An excellent summary of the general features of nodular sillimanite rocks is provided by Losert (1968). These rocks generally consist of a sillimanite + quartz nodule, surrounded by a biotite-rich selvage, set in a matrix of K-feldspar, biotite and quartz. It is common for late muscovite to partially replace the sillimanite + quartz nodule and matrix feldspar. Good photographs and illustrations of the outcrop, hand specimen and thin section features of nodular sillimanite rocks from the Park Range in Colorado were provided by Snyder *et al.* (1988, Figs. 7 through 12).

Because the sillimanite + quartz nodule appears to have grown at the expense of K-feldspar in the matrix surrounding the nodule, Losert (1968) and Eugster (1970) interpreted these features to be indicative of a metasomatic process that leached K

FIG. 6. Calculated reaction-model for textures developed where sillimanite nodules grow in a rock containing muscovite and K-feldspar. a) Starting configuration showing minerals involved in the overall reaction. The chemical potentials of all components are fixed at constant values by the matrix assemblage, so that no material transport takes place. b) Local reactions, mineral modes and segregation morphology that develop from the starting configuration. The same amount of biotite is consumed in the interior of the sillimanite segregation as is produced in the outer part of the sillimanite segregation. There is no net gain or loss of biotite at the scale of a hand specimen. The dotted line shows location of the area enlarged for Figure 6c. c) Material transport, sources and sinks along a profile from the sillimanite core (left) to the matrix (right). Notation conventions are the same as in 3c.

from the rock. Neither of these studies provided an explanation of the biotite-rich selvages around the nodules. Another alternative, which can explain the biotite-rich selvages around the nodules (Kerrick 1990, p. 323), is that biotite was acting as a catalyst for the reaction:

$$1.0\ Ms + 1.0\ Qtz \rightarrow 1.0\ Sil + 1.0\ Kfs + 1.0\ Wa \quad (17)$$

In this case, the formation of sillimanite nodules would be controlled by temperature and pressure, rather than metasomatism.

To quantitatively model the textures produced by reaction (17), consider a rock composed of 20% biotite, 30% muscovite, 45% quartz, 5% K-feldspar and a water-rich grain-boundary phase that is undergoing isobaric heating at low pressure. This assemblage is stable under a wide range of conditions in the greenschist and amphibolite facies, so that not much would happen in the rock until reaction (17) is overstepped. The configuration of the rock shortly after sillimanite has nucleated is shown in Figure 6a. There is no transport through the matrix around the growing sillimanite because the chemical potential gradients of all components in the matrix are forced to be zero at fixed T and P by the Gibbs–Duhem equations for the matrix phases and the fact that sillimanite is a linear combination of these phases. This means that the sillimanite-forming reactions in a volume of rock surrounded by matrix must sum to reaction (17). Eventually, this reaction will consume all of the muscovite or quartz in the volume of rock adjacent to the sillimanite, producing a quartz-free (Qtz) or muscovite-free (Ms) mantle. For the mineral modes of the rock shown in Figure 6a, muscovite is consumed first, and the material transport to and from the growing sillimanite will be controlled by local equilibrium with biotite + K-feldspar + quartz + water. Application of the same approach used to obtain reaction (2) (see Appendix) allows calculation of the reaction taking place in the volume of rock surrounded by the (Ms) mantle:

$$1.7\ AlO_{3/2} + 0.1\ Qtz + 0.3\ Kfs \rightarrow 1.0\ Sil + 0.3\ KO_{1/2} \quad (18)$$

Subtracting reaction (18) from reaction (17) gives the reaction at the (Ms) mantle – matrix boundary:

$$0.3\ KO_{1/2} + 1.0\ Ms + 0.9\ Qtz \rightarrow 1.3\ Kfs + 1.7\ AlO_{3/2} + 1.0\ Wa \quad (19)$$

Reaction (19) is then used with the matrix modes to calculate the modes in the (Ms) mantle: 21% biotite, 42% quartz and 37% K-feldspar. For these modes, reaction (18) will consume all the K-feldspar near the growing sillimanite, leaving transport to and from the site of sillimanite reaction controlled by local equilibrium with biotite + quartz + water in the (MsKfs) mantle. The only reaction among sillimanite, biotite, quartz and water allowed by this constraint is reaction (2). Subtraction of reaction (2) from reaction (18) gives the reaction at the (MsKfs) mantle – (Ms) mantle boundary:

$$0.21\ FeO + 0.07\ Wa + 0.3\ Kfs \rightarrow 0.07\ Bt + 0.69\ Qtz + 0.23\ KO_{1/2} + 0.23\ AlO_{3/2} \quad (20)$$

The two local reactions and morphology inside of the part of the segregation surrounded by the (MsKfs) mantle are the same as for the sillimanite segregations discussed in previous sections. If reaction (2) consumes biotite first, a (MsKfsBt) mantle will form, and the reactions at the inner and outer margins of this mantle will be (3) and (6), respectively. If reaction (2) consumes quartz first, a (MsKfsQtz) mantle will form, and the reactions at the inner and outer margins of this mantle will be (4) and (7), respectively. For the matrix modes given in the example shown in Figure 6b, biotite is consumed, creating a (MsKfsBt) mantle. As discussed at the end of the Appendix, there are large changes in volume associated with reactions (3) and (6) . This may explain why it is common for the (MsKfsBt) mantle to be poorly developed in many rocks containing nodular sillimanite. A more common morphology is for quartz and sillimanite to form a nodular intergrowth, which forms as reaction (2) consumes biotite and quartz in the (MsKfs) mantle. The quartz in the sillimanite nodule is quartz from the (MsKfs) mantle that remained when reaction (2) consumed the last biotite.

The amount of biotite consumed in the interior of the segregation shown in Figure 6b is equal to the amount produced in the outer part of the segregation. Also, note that the width of the biotite-rich (MsKfs) mantle shown in Figure 6b is much narrower than the (Ms) mantle with the same

FIG. 7. Growth of multiple nodules of sillimanite due to the thermal decomposition of muscovite. a) Reaction is partially completed. Muscovite-free mantles have begun to coalesce, but some enclaves of muscovite-bearing matrix are still present in the regions most distant from sillimanite. b) Reaction is complete. All muscovite has been consumed, leaving sillimanite nodules with a biotite-rich selvage (MsKfs mantle) in a matrix of K-feldspar + biotite + quartz that represents coalesced (Ms) mantles produced during growth of sillimanite.

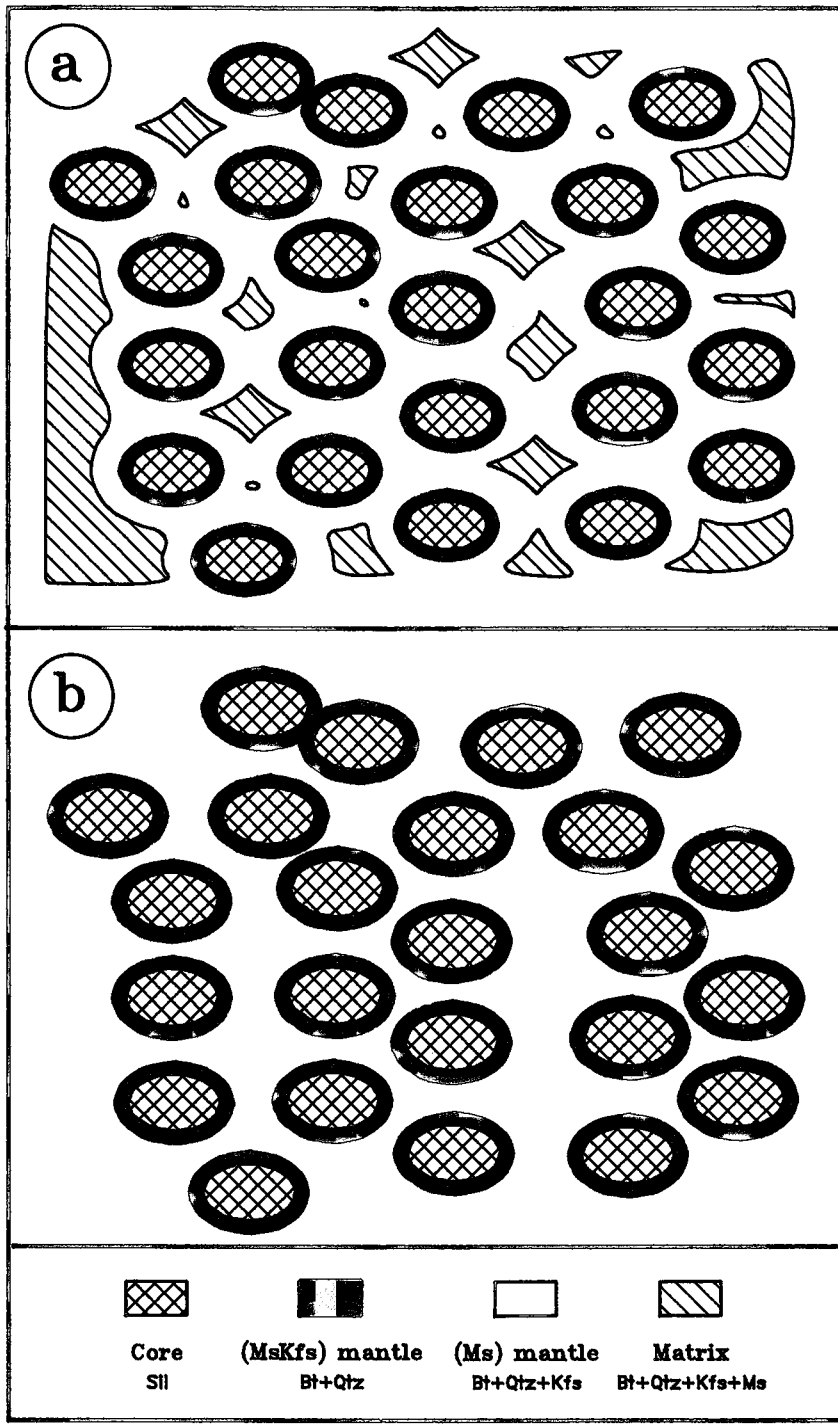
a
b
Core
Sil
(MsKfs) mantle
Bt+Qtz
(Ms) mantle
Bt+Qtz+Kfs
Matrix
Bt+Qtz+Kfs+Ms

assemblage in Figure 3b. This occurs because the presence of K-feldspar fixes the chemical potential gradient of Fe at zero in the (Ms) mantle of the segregation shown in Figure 6b, limiting the transport of Fe to a very narrow zone (Fig. 6c). The constraint on the transport of Fe restricts the local reactions involving biotite to the same narrow region of the segregation, producing a distinct biotite-rich selvage. This may explain why biotite-rich selvages around sillimanite are more easily recognized in K-feldspar-bearing rocks. As with the previous examples, failure to recognize the local reactions producing biotite at the expense of K-feldspar will lead to the erroneous conclusions that biotite was being consumed in the whole-rock reaction, and that Fe and K were being removed from the rock by a metasomatic process.

A more subtle error is possible if reaction (17) has gone to completion. In this case, all the muscovite is consumed in the rock. This process is schematically depicted on the hand specimen or outcrop scale in Figure 7. The growth of multiple nodules in a rock leads to the development of muscovite-free mantles that eventually coalesce, leaving isolated enclaves of the original matrix (Fig. 7a). When the process is complete, all of the muscovite has been consumed, and the rock is composed of sillimanite + quartz nodules with biotite-rich selvages set in a matrix of K-feldspar, biotite and quartz (Fig. 7b). In Figure 7b, there is little textural evidence to suggest that muscovite was ever in the rock. Failure to realize that the region around the segregation in Figure 7b is actually a mantle produced by the growth of sillimanite would lead to the interpretation that the nodules developed in a rock containing only K-feldspar, quartz and biotite. A logical (but incorrect) conclusion that would be drawn from this interpretation is that sillimanite must have been produced by a mechanism involving alkali leaching due to acid metasomatism.

Conclusions

When sillimanite grows in micaceous rocks, the constraints imposed on material transport by the matrix assemblage generally produce reaction mechanisms that use biotite as a mineral catalyst. In many cases, there is clear textural evidence for local reactions that consume biotite, whereas evidence for other local reactions that produce biotite is subtle and difficult to recognize. This type of reaction mechanism is responsible for the biotite-rich selvages observed in many rocks that contain nodular sillimanite. Failure to properly account for all reactions that took place during the growth of sillimanite in rocks with these textures can result in erroneous conclusions about the P–T–X path of metamorphism. Careful analysis of the spatial relationships of minerals in a rock, combined with principles of irreversible thermodynamics, can be used to determine the overall reaction that took place in the rock and to gain insight into the controls of metamorphism.

Acknowledgements

Comprehensive reviews by Saki Olsen and Ray Joesten greatly improved an early version of this manuscript. R. F. Martin and D. L. Foster made helpful editorial suggestions. Calculations for this work were performed using computer equipment purchased with funds provided by a grant from the Amoco Foundation.

References

Bailes, A.H. & McRitchie, W.D. (1978): The transition from low to high grade metamorphism in the Kisseynew Sedimentary Gneiss Belt, Manitoba. *Geol. Surv. Can., Pap.* **78-10**, 155-177.

Brady, J.B. (1975): Reference frames and diffusion coefficients. *Am. J. Sci.* **275**, 954-983.

Briggs, W.D. & Foster, C.T. (1989): An irreversible thermodynamic model of reaction mechanisms in sillimanite schists, File Lake, Manitoba. *Geol. Assoc. Can. - Mineral. Assoc. Can., Program Abstr.* **14**, A6.

Carmichael, D.M. (1969): On the mechanism of prograde metamorphic reactions in quartz-bearing pelitic rocks. *Contrib. Mineral. Petrol.* **20**, 244-267.

_____ (1987): Induced stress and secondary mass transfer: thermodynamic basis for the tendency toward constant-volume constraint in diffusion metasomatism. *In* Chemical Transport in Metasomatic Processes (H.C. Helgeson, ed.). D. Reidel, Dordrecht, Holland (239-264).

Chinner, G.A. (1961): The origin of sillimanite in Glen Cova, Angus. *J. Petrol.* **2**, 312-323.

Eugster, H.P. (1970): Thermal and ionic equilibria among muscovite, K-feldspar and aluminosilicate assemblages. *Fortschr. Mineral.* **47**, 106-123.

_____ & Baumgartner, L. (1987): Mineral solubilities and speciation in supercritical metamorphic fluids. *In* Thermodynamic Modeling of Geological Materials: Minerals, Fluids, and Melts (I.S.E. Carmichael & H.P. Eugster, eds.). *Rev. Mineral.* **17**, 367-403.

Fisher, G.W. (1975): The thermodynamics of diffusion controlled metamorphic processes. *In* Mass

Transport Phenomena in Ceramics (A.R. Cooper & A.H. Heuer, eds.). Plenum Press, New York (111-122).

_____ (1977): Nonequilibrium thermodynamics in metamorphism. *In* Thermodynamics in Geology (D.G. Fraser, ed.). D. Reidel, Dordrecht, Holland (381-403).

_____ (1978): Rate laws in metamorphism. *Geochim. Cosmochim. Acta* **42**, 1035-1050.

FOSTER, C.T., JR. (1977): Mass transfer in sillimanite-bearing pelitic schists near Rangeley, Maine. *Am. Mineral.* **62**, 727-746.

_____ (1981): A thermodynamic model of mineral segregations in the lower sillimanite zone near Rangeley, Maine. *Am. Mineral.* **66**, 260-277.

_____ (1982a): Textural variation of sillimanite segregations. *Can. Mineral.* **20**, 379-392.

_____ (1982b): A model for sillimanite segregations and staurolite pseudomorphs in plagioclase-rich, muscovite-poor pelites. *Geol. Assoc. Can. - Mineral. Assoc. Can., Program Abstr.* **7**, A49.

_____ (1983): Thermodynamic models of biotite pseudomorphs after staurolite. *Am. Mineral.* **68**, 389-397.

_____ (1986): Thermodynamic models of reactions involving garnet in a sillimanite/staurolite schist. *Mineral. Mag.* **50**, 427-439.

_____ (1990a): Control of material transport and reaction mechanisms by metastable mineral assemblages: an example involving kyanite, sillimanite, muscovite and quartz. *In* Fluid - Mineral Interactions: a Tribute to H.P. Eugster (R.J. Spencer & I-Ming Chou, eds.). *The Geochemical Society, Spec. Publ.* **2**, 121-132.

_____ (1990b): The role of biotite as a catalyst in reaction mechanisms that form fibrolite. *Geol. Assoc. Can. - Mineral. Assoc. Can., Program Abstr.* **15**, A40.

HELGESON, H.C., DELANY, J.M., NESBITT, H.W. & BIRD, D.K. (1978): Summary and critique of the thermodynamic properties of rock-forming minerals. *Am. J. Sci.* **278A**.

HIETANEN, A. (1963): Metamorphism of the Belt Series in the Elk River - Clarkia area, Idaho. *U. S. Geol. Surv., Prof. Pap.* **344C**.

KERRICK, D.M. (1987): Fibrolite in contact aureoles of Donegal, Ireland. *Am. Mineral.* **72**, 240-254.

_____ (1990): The Al_2SiO_5 polymorphs. *Rev. Mineral.* **22**.

_____ & WOODSWORTH, G.J. (1989): Aluminum silicates in the Mount Raleigh pendant, British Columbia. *J. Metamorph. Geol.* **7**, 547-563.

KNAPP, R. (1989): Spatial and temporal scales of local equilibrium in dynamic fluid - rock systems. *Geochim. Cosmochim. Acta* **53**, 1955-1964.

KRETZ, R. (1983): Symbols for rock-forming minerals. *Am. Mineral.* **68**, 277-279.

LOSERT, J. (1968): On the genesis of nodular sillimanite rocks. *23rd Intern. Geol. Congress.* **4**, 109-122.

SCHNEIDERMAN, J.S. (1990): Use of reaction space in depicting polymetamorphic histories. *Geology* **18**, 350-353.

SNYDER, G.L., BRANDT, E.L. & SMITH, V.C. (1988): Precambrian petrochemistry of the northern Park Range and its implications for studies of crustal derivation. *U.S. Geol. Surv., Prof. Pap.* **1343**.

SPEAR, F.S. (1988): The Gibbs method and Duhem's theorem: the quantitative relationships among P, T, chemical potential, phase composition and reaction progress in igneous and metamorphic systems. *Contrib. Mineral. Petrol.* **99**, 249-256.

THOMPSON, J.B., JR. (1982): Reaction space: an algebraic and geometric approach. *In* Characterization of Metamorphism through Mineral Equilibria (J.M. Ferry, ed.). *Rev. Mineral.* **10**, 33-52.

VERNON, R.H. (1979): Formation of late sillimanite by hydrogen metasomatism (base-leaching) in some high-grade gneisses. *Lithos* **12**, 143-152.

WALTHER, J.V. (1986): Mineral solubilities in supercritical H_2O solutions. *Pure and Applied Chem.* **58**, 1585-1598.

_____ & WOOD, B.J. (1986): Mineral - fluid reaction rates. *In* Fluid - Rock Interactions During Metamorphism (J.V. Walther & B.J. Wood, eds.). Springer-Verlag, New York (194-211).

WOODLAND, A.B. & WALTHER, J.V. (1987): Experimental determination of the solubility of the assemblage paragonite, albite, and quartz in supercritical H_2O. *Geochim. Cosmochim. Acta* **51**, 365-372.

YARDLEY, B.W.D. (1977): The nature and significance of the mechanism of sillimanite growth in the Connemara Schists, Ireland. *Contrib. Mineral. Petrol.* **65**, 53-58.

Received December 17, 1990, revised manuscript accepted September 10, 1991.

APPENDIX: CALCULATION OF REACTIONS

The details of calculations used to obtain reactions (1) through (7) are shown below. The approach presented here follows the algebraic substitution method of Fisher (1975). Readers familiar with linear algebra may wish to refer to Foster (1981, 1982a), where a matrix approach is used to solve similar equations.

Reaction (1)

The reaction that takes place where sillimanite grows in a matrix of muscovite, biotite, quartz and water under conditions of local equilibrium can be calculated using thermodynamic principles that link the reaction to material transport driven by chemical potential gradients in the matrix. In the simplest case, where cross terms in the diffusion coefficients are unimportant, the magnitude of the flux (J_i) of a component in the matrix is related to the magnitude of the chemical potential gradient ($\nabla\mu_i$) of the component by a single thermodynamic diffusion-coefficient (L_i):

$$J_i = -L_i \bullet \nabla\mu_i.$$

The μ_i in the matrix are constrained by local equilibrium to lie along the metastable portion of the Bt + Qtz + Ms line shown in Figure 2. This means that $(\Delta\mu_{AlO_{3/2}}/\Delta\mu_{KO_{1/2}})$ and $(\Delta\mu_{FeO}/\Delta\mu_{KO_{1/2}})$ in the matrix are fixed at -0.334 and -0.225, respectively. The magnitudes of the relative fluxes of components through the matrix can be calculated from these ratios if the L_i are known. Use of values of L_i ratios from Foster (1981) gives:

$$\frac{J_{AlO_{3/2}}}{J_{KO_{1/2}}} = \frac{-L_{AlO_{3/2}}}{-L_{KO_{1/2}}} \cdot \frac{\nabla\mu_{AlO_{3/2}}}{\nabla\mu_{KO_{1/2}}} = \frac{-5.9}{-1} \cdot (-0.334) = -1.971$$

and

$$\frac{J_{FeO}}{J_{KO_{1/2}}} = \frac{-L_{FeO}}{-L_{KO_{1/2}}} \cdot \frac{\nabla\mu_{FeO}}{\nabla\mu_{KO_{1/2}}} = \frac{-2.6}{-1} \cdot (-0.225) = -0.585$$

These ratios mean that 0.585 moles of FeO and 1.97 moles of $AlO_{3/2}$ are supplied to the reaction site for every mole of $KO_{1/2}$ that leaves. The number of moles (R_j) of biotite [$KFe_3AlSi_3O_{10}(OH)_2$], muscovite [$KAl_3Si_3O_{10}(OH)_2$] and sillimanite (Al_2SiO_5) produced ($R_j > 0$) or consumed ($R_j < 0$) in the reaction are related to the fluxes in the matrix:

$$R_{biotite} = \frac{-J_{FeO}}{3}$$

$$R_{muscovite} = -J_{KO_{1/2}} - R_{biotite}$$

and

$$R_{sillimanite} = \frac{-J_{AlO_{3/2}}}{2} - \frac{3R_{muscovite}}{2} - \frac{R_{biotite}}{2}$$

The sign convention for the fluxes has been chosen so that diffusion away from the segregation center is positive. Setting $J_{KO_{1/2}} = -1$ allows the proportions of biotite, muscovite and sillimanite taking part in the reaction to be determined:

$$\frac{R_{muscovite}}{R_{biotite}} = \frac{1.0 + \frac{0.585}{3}}{\frac{-0.585}{3}} = -6.13$$

and

$$\frac{R_{biotite}}{R_{sillimanite}} = \frac{\frac{-0.585}{3}}{\frac{-1.971}{2} - \left(3 \cdot \frac{1 + (0.585/3)}{2}\right) - \frac{0.585}{3}} = 0.07$$

Assignment of the amount of sillimanite produced equal to one mole ($R_{sillimanite} = 1.0$) gives the stoichiometric coefficients for reaction (1).

The diffusion coefficients derived by Foster (1981) were used to calculate reaction (1) because they appear to be valid in a wide variety of amphibolite-facies pelites (Briggs & Foster 1989, Foster 1982a, b, 1983, 1986). However, as shown in Figure 8, the basic form of reaction (1) is insensitive to the relative values of the K, Fe, and Al coefficients of diffusion. Variation of the diffusion coefficient ratios does have an important effect on the ΔV of reaction (see captions of Figs. 8a, 8b, 8c). Use of ratios of diffusion coefficients from Foster (1981) to calculate the stoichiometry of reaction (1) results in a volume change of less than 1% among the solid phases.

Reaction (2)

The values of μ_i in the (Ms) mantle must lie on the metastable Bt + Qtz surface shown on Figure 2. Therefore, the $\nabla\mu_i$ within the mantle are constrained by the Gibbs–Duhem equations for biotite and quartz so that:

$$-\nabla\mu_{KO_{1/2}} = \nabla\mu_{AlO_{3/2}} + 3\nabla\mu_{FeO} + 3\nabla\mu_{SiO_2}$$

and

$$\nabla\mu_{SiO_2} = 0$$

Substituting $\nabla\mu_i = -J_i/L_i$ into the first equation gives:

$$\frac{J_{KO_{1/2}}}{L_{KO_{1/2}}} = \frac{-J_{AlO_{3/2}}}{L_{AlO_{3/2}}} - \frac{3J_{FeO}}{L_{FeO}} - \frac{3J_{SiO_2}}{L_{SiO_2}} \qquad (A)$$

Biotite is the only K- and Fe-bearing phase present at the inner mantle boundary, so that Fe and K must both be produced or consumed by the reaction at this boundary in a ratio of 1 to 3. This requires that $3J_{KO_{1/2}} = J_{FeO}$ in the (Ms) mantle. The absence of a chemical potential gradient of silica fixes J_{SiO_2} to be equal to 0. Substitution of these relationships into equation (A) gives:

$$\frac{J_{KO_{1/2}}}{L_{KO_{1/2}}} = \frac{-J_{AlO_{3/2}}}{L_{AlO_{3/2}}} - \frac{9J_{KO_{1/2}}}{L_{FeO}}$$

A rearrangement of this equation gives a relationship among the magnitudes of the K and Al fluxes:

$$\frac{J_{KO_{1/2}}}{L_{KO_{1/2}}} + \frac{9J_{KO_{1/2}}}{L_{FeO}} = \frac{-J_{AlO_{3/2}}}{L_{AlO_{3/2}}}$$

A division by the magnitude of the K flux and rearranging gives the ratio of Al to K flux in the (Ms) mantle:

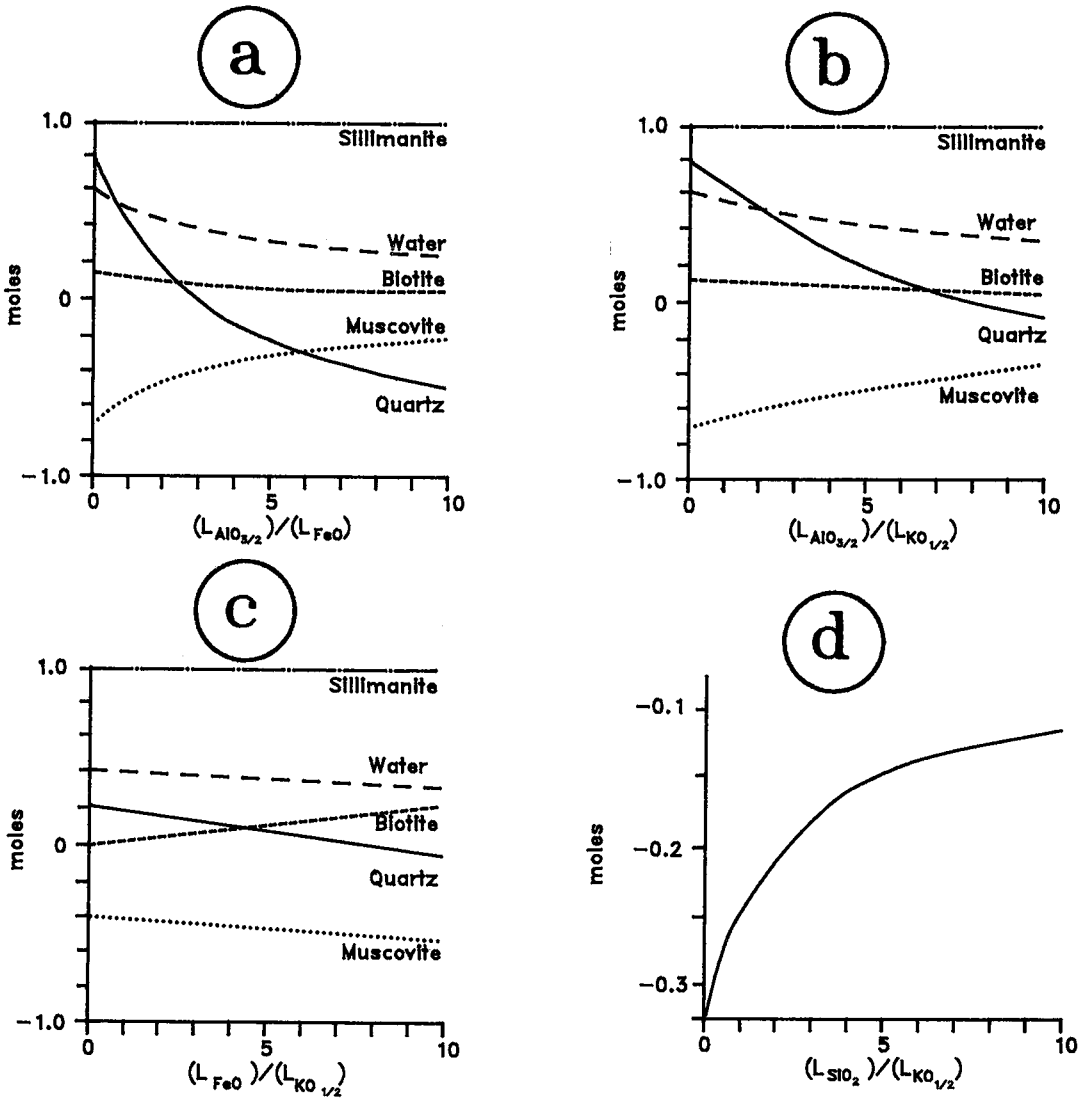

FIG. 8. The effect of L coefficient ratios on the stoichiometry of reactions (1) and (4). Positive numbers on the vertical axis indicate that the phase is produced in the reaction, whereas negative numbers indicate that the phase is consumed in the reaction. The stoichiometric coefficients of biotite and sillimanite remain positive, and the stoichiometric coefficient of muscovite remains negative, in reaction (1) even though the ratios of diffusion coefficients are varied over two orders of magnitude. a) Stoichiometry of reaction (1) as a function of $(L_{AlO_{3/2}})/(L_{FeO})$. The ratios of diffusion coefficients for other components were held constant at the values taken from Foster (1981). The volume change of reaction calculated with the lowest L ratio shown on this graph was −2%. The volume change of the reaction calculated with the largest L ratio on this graph was +11%. b) Stoichiometry of reaction (1) as a function of $(L_{AlO_{3/2}})/(L_{KO_{1/2}})$. Ratios of diffusion coefficients for other components were held constant at the values taken from Foster (1981). The volume change of the reaction calculated with the lowest L ratio shown on this graph was −13%. The volume change of the reaction calculated with the largest L ratio on this graph was +13%. c) Stoichiometry of reaction (1) as a function of $(L_{FeO})/(L_{KO_{1/2}})$. Ratios of diffusion coefficients for other components were held constant at the values taken from Foster (1981). The volume change of the reaction calculated with the lowest L ratio shown on this graph was −13%. The volume change of the reaction calculated with the largest L ratio on this graph was +40%. d) Variation of the stoichiometric coefficient of biotite in reaction (4) as a function of $(L_{SiO_2})/(L_{KO_{1/2}})$. The ratios of diffusion coefficients for other components were held constant at the values taken from Foster (1981). A value of $(L_{SiO_2})/(L_{KO_{1/2}}) = 0.1$ gives a reaction in which volume is conserved among the solid phases.

$$\frac{L_{AlO_{3/2}}}{L_{KO_{1/2}}} + \frac{9L_{AlO_{3/2}}}{L_{FeO}} = \frac{-J_{AlO_{3/2}}}{J_{KO_{1/2}}} \quad (B)$$

The amount of biotite reacting at the inner boundary of the muscovite-free mantle is given by:

$$R_{biotite} = -J_{KO_{1/2}} \quad (C)$$

and the amount of sillimanite is given by:

$$R_{sillimanite} = \frac{-J_{AlO_{3/2}}}{2} - \frac{R_{biotite}}{2}$$

A division by $R_{biotite}$, substitution with equations (B), (C), and use of the ratios of L_i taken from Foster (1981) give the proportions of minerals taking part in the reaction in the portion of the segregation surrounded by the muscovite-free mantle:

$$\frac{R_{sillimanite}}{R_{biotite}} = \frac{1}{2}\left[\frac{-J_{AlO_{3/2}}}{R_{biotite}} - 1\right] = \frac{1}{2}\left[\frac{-J_{AlO_{3/2}}}{-J_{KO_{1/2}}} - 1\right]$$

$$= -\frac{1}{2}\left[\frac{L_{AlO_{3/2}}}{L_{KO_{1/2}}} + \frac{9L_{AlO_{3/2}}}{L_{FeO}} + 1\right] = -\frac{1}{2}\left[\frac{5.9}{1} + 9\cdot\left[\frac{5.9}{2.6}\right] + 1\right] = -13.66$$

Setting $R_{sillimanite}$ equal to 1.0 and a balancing of SiO_2 and H_2O with quartz and water, respectively give the stoichiometric coefficients for reaction (2).

Reaction (3)

Sillimanite and quartz are the only phases inside of the (MsBt) mantle. The amount of sillimanite and quartz taking part in the reaction is related to the flux of Al and Si through the (MsBt) mantle: $R_{sillimanite} = -J_{AlO_{3/2}}$ and $R_{quartz} = -R_{sillimanite} - J_{SiO_2}$. Since quartz is present in the (MsBt) mantle, μ_{SiO_2} is constant, which fixes J_{SiO_2} equal to 0. Thus, $R_{quartz} = -R_{sillimanite}$. Setting $R_{sillimanite}$ equal to 1.0 gives the stoichiometry for reaction (3).

Reaction (4)

Biotite and sillimanite are the only solid phases available inside of the (MsQtz) mantle, so that the magnitude of the flux terms in equation (A) is related to the amounts of sillimanite and biotite reacting in the portion of the segregation surrounded by the (MsQtz) mantle: $R_{biotite} = (-J_{KO_{1/2}})$, $3R_{biotite} = (-J_{FeO})$, $2R_{sillimanite} + R_{biotite} = -J_{AlO_{3/2}}$, and $R_{sillimanite} + 3R_{biotite} = -J_{SiO_2}$. Substitution of these relations into equation (A) and rearranging gives:

$$\frac{R_{biotite}}{R_{sillimanite}} = \frac{-2\cdot\frac{L_{KO_{1/2}}}{L_{AlO_{3/2}}} - 3\cdot\frac{L_{KO_{1/2}}}{L_{SiO_2}}}{1 + \frac{L_{KO_{1/2}}}{L_{AlO_{3/2}}} + 9\cdot\frac{L_{KO_{1/2}}}{L_{FeO}} + 9\cdot\frac{L_{KO_{1/2}}}{L_{SiO_2}}}.$$

Use of the diffusion coefficient ratios of Foster (1981) gives the amount of biotite that reacts when one mole of sillimanite is produced as a function of the ratio of the diffusion coefficients for K and Si:

$$= \frac{-2\cdot\frac{1.0}{5.9} - 3\cdot\frac{L_{KO_{1/2}}}{L_{SiO_2}}}{1 + \frac{1.0}{5.9} + 9\cdot\frac{1.0}{2.6} + 9\cdot\frac{L_{KO_{1/2}}}{L_{SiO_2}}}$$

Figure 8d shows that the reaction is relatively insensitive to the ratio of the thermodynamic diffusion coefficients for K and Si. Biotite is always consumed where sillimanite grows. Variation in the ratio of the diffusion coefficients by two orders of magnitude changes the amount of biotite consumed by a factor of three. Textural evidence suggests that this reaction proceeds at nearly constant volume (*e.g.*, Kerrick 1990, Fig. 9.11); therefore, the correct $L_{SiO_2}/L_{KO_{1/2}}$ value should be about 0.1, the value that gives the reaction where the volume of sillimanite produced equals the volume of biotite consumed. This value was used to calculate reaction (4).

Reaction (5)

The reaction at the matrix – (Ms) mantle interface is obtained by subtracting reaction (2) from reaction (1). Reaction (2) is the sum of the local reactions taking place inside the portion of the segregation surrounded by the (Ms) mantle. Reaction (1) is the sum of all the local reactions taking place in the segregation as a whole. The local reaction at the matrix – (Ms) mantle interface is included in reaction (1), but not in reaction (2). Therefore, the difference between reaction (1) and reaction (2) is reaction (5).

Reaction (6)

The reaction at the (Ms) mantle – (MsBt) mantle interface is obtained by subtracting reaction (3) from reaction (2). Reaction (3) is the sum of the local reactions taking place inside the portion of the segregation surrounded by the (MsBt) mantle. Reaction (2) is the sum of the local reactions taking place inside the portion of the segregation surrounded by the (Ms) mantle. The reaction at the (Ms) mantle – (MsBt) mantle interface is included in reaction (2) but not in reaction (3). Therefore, the difference between reaction (2) and reaction (3) is reaction (6).

Reaction (7)

The reaction at the (MsQtz) mantle – (Ms) mantle interface is obtained by subtracting reaction (4) from reaction (2). Reaction (4) is the sum of the local reactions taking place in the portion of the segregation surrounded by the (MsQtz) mantle. Reaction (2) is the sum of the local reactions taking place in the portion of the segregation surrounded by the (Ms) mantle. The reaction at the (MsQtz) mantle – (Ms) mantle interface is included in reaction (2) but not in reaction (4). Therefore, the difference between reaction (2) and reaction (4) is reaction (7).

Calculation of mineral modes and mantle volumes for Figure 3

If sillimanite grows in a matrix composed of 20% biotite, 30% muscovite, and 50% quartz (Fig. 3a), the amount of matrix that is consumed by reaction (5) can be calculated by determining the amount of matrix that contains 0.45 moles of muscovite. For the modes given, this amounts to 208 cm^3 of matrix. In addition to the muscovite, this volume of matrix contains 0.27 moles of biotite and 4.52 moles of quartz. When reaction (5) has consumed this amount of matrix, it will have consumed all of the muscovite and converted the matrix to a mantle

composed of the original amounts of biotite (0.27 moles) and quartz (4.52 moles) plus the biotite (0.14 moles) and quartz (0.93 moles) made by reaction (5). The volume of biotite and quartz in the mantle is obtained by multiplying the molar amounts by the appropriate molar volumes. Thus, for quartz, (4.52 + 0.93) moles • 23 cm^3/mole = 125 cm^3, and for biotite, (0.27 + 0.14) moles • 154 cm^3/mole = 63 cm^3. Addition of the volume of biotite to the volume of quartz gives the total volume of the mantle (188 cm^3) that was produced from the 208 cm^3 of matrix and allows calculation of the biotite and quartz modes in the (Ms) mantle, 34% and 66%, respectively.

The molar ratio of quartz to biotite in the (Ms) mantle is larger than 11, which indicates that a (MsBt) mantle forms where reaction (2) consumes some of the (Ms) mantle created by reaction (5) and uses up all of the biotite. When a thin (MsBt) mantle is established, reaction (6) begins to convert (Ms) mantle to (MsBt) mantle. The volume of the (Ms) mantle consumed by reaction (6) is the amount that contains 0.07 moles of biotite: (0.07 • 154)/0.34 = 32 cm^3. The volume of (MsBt) mantle produced by reaction (6) is composed of the quartz in the 32 cm^3 of (Ms) mantle consumed (0.92 moles) plus the 0.21 moles of quartz produced by reaction (6): (0.92 + 0.21) • 23 = 26 cm^3. Reaction (3) consumes 23 cm^3 of the (MsBt) mantle to make 1 mole (50 cm^3) of sillimanite in the center of the segregation. The difference between the amount of (MsBt) mantle made by reaction (6) and consumed by reaction (3) gives the volume of the (MsBt) mantle around the sillimanite core: 26 – 23 = 3 cm^3. The large change in volume (+27 cm^3) produced by reaction (3) at the sillimanite core – (MsBt) mantle interface may generate strain-induced dislocations that could be responsible for the nucleation front of fibrolite needles that commonly penetrates quartz crystals in the (MsBt) mantle near sillimanite (Foster 1982a, Fig. 6). The gain in volume at this boundary is almost exactly matched by the sum of volume losses produced by the matrix – (Ms) mantle reaction (–20 cm^3) and the (Ms) mantle – (MsBt) mantle reaction (–6 cm^3). For this reason, it is difficult to assess whether the calculated losses in volume are real or if they are compensated for by redistribution of SiO_2 due to chemical potential gradients in SiO_2 imposed by stress gradients in quartz, as suggested by Carmichael (1987).

The volumes of the core and mantles enclosed by the each reaction surface are added together to calculate the radius of the lines showing the mantle boundaries in Figure 3b. The shape of the segregation volume used for this calculation is an ellipsoid flattened in the plane of foliation. This shape is common in natural specimens, in which the diameter of a sillimanite nodule is correlated with the number of grain boundaries in a given direction. This suggests that the growth rate of a segment of reaction interface is proportional to the number of grain boundaries available to transport components to and from the site of reaction.